Efficient light coupling between dielectric slot waveguide and plasmonic slot waveguide

Article *in* Optics Letters · March 2010

DOI: 10.1364/OL.35.000649 · Source: PubMed

4 authors:

Ruoxi Yang
Seagate Technology
18 PUBLICATIONS **205** CITATIONS
SEE PROFILE

Rami A. Wahsheh
Princess Sumaya University for Technology
23 PUBLICATIONS **158** CITATIONS
SEE PROFILE

Zhaolin Lu
Rochester Institute of Technology
64 PUBLICATIONS **657** CITATIONS
SEE PROFILE

Mustafa Abushagur
Rochester Institute of Technology
127 PUBLICATIONS **653** CITATIONS
SEE PROFILE

Efficient light coupling between dielectric slot waveguide and plasmonic slot waveguide

Ruoxi Yang, Rami A. Wahsheh, Zhaolin Lu,* and Mustafa A. G. Abushagur

Microsystems Engineering, Kate Gleason College of Engineering, Rochester Institute of Technology, Rochester, New York 14623, USA

**Corresponding author: zxleen@rit.edu*

Received August 19, 2009; revised December 16, 2009; accepted January 18, 2010; posted January 25, 2010 (Doc. ID 115977); published February 22, 2010

An efficient coupler between a dielectric waveguide and a plasmonic metal–insulator–metal (MIM) waveguide is proposed, modeled, fabricated, and characterized. Based on the platform of a silicon slot waveguide, a quasi-MIM plasmonic junction is formed via e-beam lithography and lift-off process. Coupling efficiency between the silicon slot waveguide and plasmonic waveguide up to 43% is obtained after normalizing to reference waveguides at 1550 nm. This coupling scheme can be potentially used for fast optical switching and small-footprint optical modulation. © 2010 Optical Society of America

OCIS codes: 130.3120, 240.6680.

Plasmonics is revolutionizing the development of nanophotonics in every aspect at an extraordinarily fast pace. Recent breakthroughs have produced a wide range of nanoplasmonic devices that generate, guide, and detect light [1–6]. However, very few have been implemented. Currently, the challenge to integrate plasmonic devices with conventional dielectric waveguides on the same chip limits the wide applications of plasmonic devices. To this end, efficient coupling between dielectric waveguides and plasmonic waveguides is of great significance. Initially, a plasmonic waveguide was proposed with a single metal–dielectric boundary, which is still widely used [7]. However, direct excitation of surface plasmon waves on such a boundary from a dielectric waveguide or external source is inefficient owing to the mismatch of **k** vectors and field profiles of the two modes. Therefore, prism couplers [8] or grating couplers [9] are used to improve the efficiency. Because of their large size, prism couplers are not suitable for photonic integrated circuits. On the other hand, the main drawbacks of grating couplers are (i) the separation of the source and plasmonic devices on different chips, (ii) the requirement of good alignment between the source and the grating, and (iii) their narrow bandwidth.

More recently, metal–insulator–metal (MIM) or metal–dielectric–metal waveguides have been investigated and experimentally demonstrated [10–16], where light propagation is confined between two metal slabs. The ultrasmall mode size and acceptable loss of MIM waveguides have been applied to nanofocusing, too [17]. Recent numerical simulation [18] demonstrated that up to 70% efficiency can be achieved when light is coupled from a dielectric waveguide into a plasmonic waveguide. Direct fabrication of the dielectric-to-plasmonic waveguide coupler is challenging, especially considering the remaining metal on different waveguides' interface will block the wave propagation. A plasmonic junction that directly converts far-field radiation to surface waves has also been demonstrated recently [19]. The fabrication in [19] engages the use of focused ion beam twice, which requires an additional curing process. The coupler involved in [16] is formed by enclosing a dielectric waveguide into metal claddings, which is hard to be used for optical sensors and modulators. Herein, we propose a practical configuration for integrated modulator and sensor applications, which can be used to achieve high coupling efficiency between dielectric waveguides and MIM plasmonic slot waveguides.

Light propagation can be confined in a low-index region when a slot is introduced inside a single- mode dielectric waveguide [20], also known as dielectric slot waveguides. Comparison of dielectric and metal slot waveguides shows that they work for the same polarization and share a similar hyperbolic cosine mode profile, as shown in Fig. 1. Inspired by this similarity, we propose to couple light from dielectric slot waveguides into metal slot waveguides, namely, the "slot-to-slot" coupler, as shown in Fig. 2(a). Our 2D numerical study has predicted a 61% transmittance for a 500-nm-long slot-to-slot coupling in Fig. 2(b). By sweeping the slot length L, spectrum response representing the Fabry–Perot effect (similar

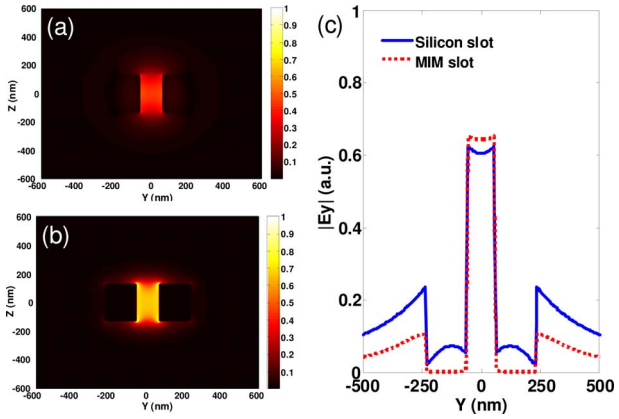

Fig. 1. (Color online) (a) Power distribution in a dielectric slot waveguide. (b) Field distribution in a metal slot waveguide. Identical power flux is assumed for (a) and (b). The power density in MIM slot is obviously higher because of the presence of metal. (c) Field ($|E_y|$) comparison [line scan from Figs. 1(a) and 1(b)] between dielectric and MIM slot. MIM slot exhibits better field confinement as expected.

0146-9592/10/050649-3/$15.00

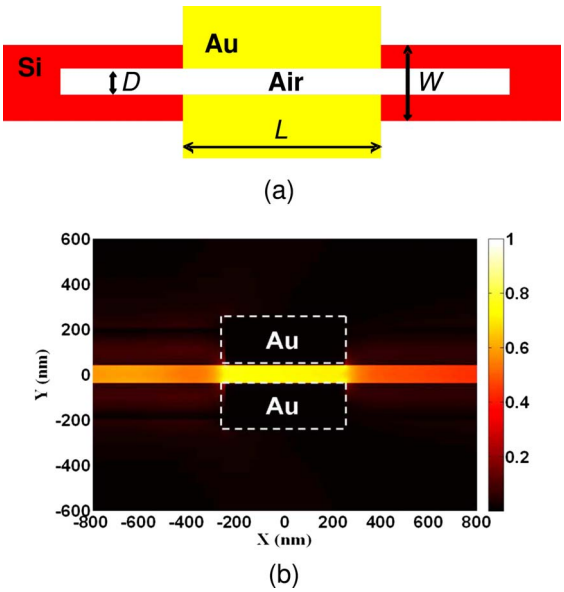

Fig. 2. (Color online) (a) Layout of slot-to-slot coupler. (b) Power distribution from 2D FDTD simulation for slot-to-slot coupler.

to that reported in [18]) is observed. From a practical view, however, the plain slot-to-slot scheme is still very hard to demonstrate on silicon-on-insulator (SOI) platform because of the requirement for very critical alignment and the deep trenches milled into a bulk metal. To overcome these difficulties, we notice that the power skin depth of metal at $\lambda = 1550$ nm is only a few nanometers. Therefore, a metal film embedded in a dielectric slot can be a good quasi-MDM waveguide as shown in Fig. 3.

The 3D structure is designed and modeled by finite-difference time-domain (FDTD) simulation packages that support nonuniform meshing and eigenmode calculation. A cross section of 260 nm by 460 nm ($W = 460$ nm) is assumed for a single-mode (SM) silicon strip waveguide that supports a fundamental TE-like mode (E vector is in the slab) for near-IR light at 1550 nm. A slot is embedded in the strip waveguide with a slot width $D = 120$ nm, as shown in Fig. 2(a). A plasmonic region with a total length of $L = 500$ nm is then formed by isotropically adding a thin layer (~ 20 nm) of gold ($\varepsilon_r = -96 + j11$) over the silicon slot, which produces an 80-nm-wide airgap, as shown in Fig. 3(a). A quasi-TE-like polarization is used to retrieve an eigenmode of the silicon slot as the simulation source. Figure 3(b) illustrates transverse electric field E_y inside the quasi-MIM slot. For $L = 500$ nm, the normalized transmission is close to 50%. From our simulation, when L keeps increasing to exceed 1.5 μm, the propagation loss dominates and transmission decreases very fast.

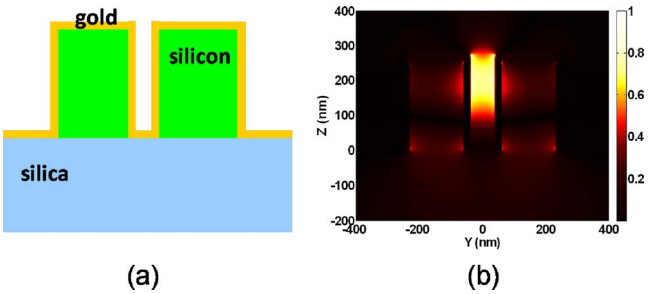

Fig. 3. (Color online) (a) Cross-section view of the quasi-MIM structure. (b) Cross-section view of the field distribution $|E_y|$ for the quasi-MIM structure from 3D FDTD simulation.

In addition to equally high-level coupling efficiency as direct coupling, a remarkable advantage of our coupler is that it can be fabricated *without using the focused ion beam*. First, electron-beam lithography (EBL) and inductively coupled plasma (ICP) etch were used to pattern a 50-μm-long and 120-nm-wide slot inside an SM silicon waveguide with a cross-section around 260 nm by 460 nm. The piece was then exposed by EBL again with bilayer PMMA for lift-off. After development a 20 μm by 500 nm (or 20 μm by 2 μm for a second design) window was opened right at the center of the 50-μm-long silicon slot, where obliquely evaporated gold was then deposited, followed by metal lift-off. The top view shown in Fig. 4(a) gives the outlook of the fabricated device with very good alignment.

To characterize the structure, we fabricated three structures altogether on an SOI wafer. The first one is an SM waveguide (with 50-μm-long slot waveguide included) without any plasmonic region, and is therefore regarded as a reference structure. Two designs with different L values (500 nm and 2 μm) are fabricated to characterize the quasi-MIM region. A tunable laser with the maximum output power of 20 mW is used as the probing source. The devices are then viewed by an IR camera working with a microscope, as given in Figs. 4(b)–4(d). There is considerable scattering when light is coupled between the dielectric strip and the dielectric slot waveguide, which accounts for a large part of insertion loss. This issue can be addressed by strip-to-slot waveguide transformers [21,22], where nearly perfect coupling can be achieved. Compared with the reference structure where no metal segments exist [Fig. 4(b)], the scat-

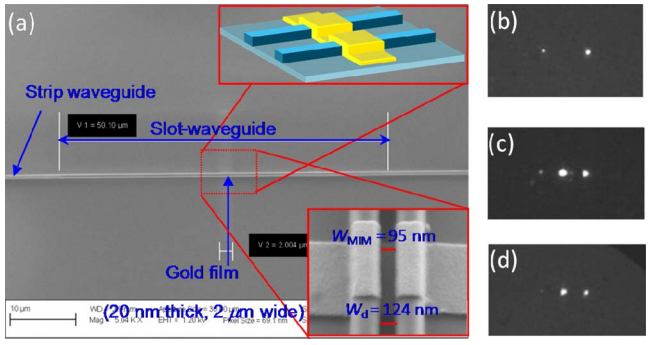

Fig. 4. (Color online) (a) Device top view with quasi-MIM region sketched (top inset) and shown by scanning electron microscope picture (bottom inset). (b) Device top view for scattering of near-IR light from a silicon slot when power is coupled from an SM silicon waveguide on the right-hand side. (c) Light scattered from a dielectric slot with 500 nm quasi-MIM. The weakened scattering compared with (a) denotes the loss introduced by the quasi-MIM region. (d) Light scattered from a dielectric slot with 2 μm quasi-MIM.

tering on the output port (the bright points on the left) seen in Figs. 4(c) and 4(d) are weaker but still obvious. In this Letter the plasmonic device is characterized by normalizing its output to that of the dielectric slot waveguide, which avoids the consideration of strip-to-slot insertion loss.

The bandwidth characterization is performed when input power is locked at 10 mW. Efficient light propagation for reference device (no MIM) is observed between 1460 nm and 1620 nm, averaged to 4 μW. Spectrum sweep is then performed for the two MIM cases. After averaging the results and looking at the power around 1550 nm, we obtain $\sim$1.7 μW output (or 43% transmission, normalized to the 4 μW output from reference) for $L=500$ nm case and $\sim$0.6 μW output (15% transmission) for $L=2$ μm case [Fig. 5]. The transmission difference between the two designs corresponds to a propagation loss of $\sim$2 dB/μm for the fabricated quasi-MIM structure. However, previous analytical study of propagation surface-plasmon modes in the MIM structure has highlighted the role of multimode interference (MMI) [23], which indicates a critical relevance between the length of waveguide and the field distribution at output. To thoroughly characterize the quasi-MIM configuration proposed, including measuring the propagation loss of unit length, a different approach considering the role of MMI is necessary and will be reported elsewhere. The broadband performance is facilitated by "funneling" of power into MIM slot [24], besides impedance match and mode overlap. The mechanism of the nanofunneling effect can be numerically studied by transmission line theory [25] or antenna theory that has been carried out for microwave region. We believe the scheme proposed here can be further optimized if the mechanism of direct coupling can be realized more thoroughly.

To summarize, we have reported the design and demonstration of an integrated coupler that combines plasmonic devices with dielectric waveguides for near-IR light. The performance of this coupler is in agreement with 3D FDTD simulation and shows efficient coupling, acceptable bandwidth, and straightforward fabrication. Based on the platform described in this Letter, plasmonic switches or modulators with an active length of only a few micrometers are expected if the propagation of SPP can be modulated in previous approaches [26].

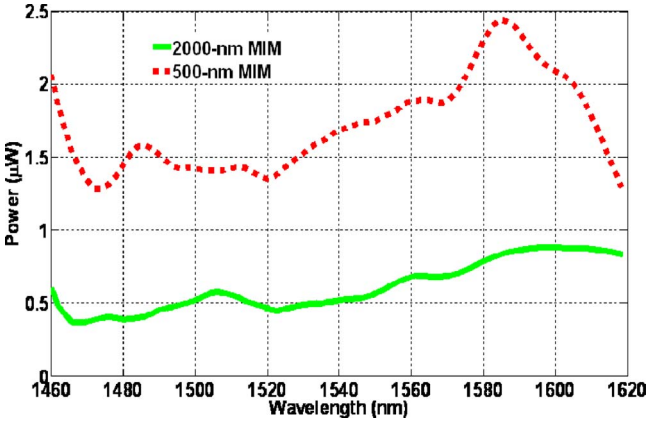

Fig. 5. (Color online) Spectrum response between 1460 nm and 1620 nm of two quasi-MIM designs. The averaged power is approximately 1.7 μW for the 500 nm case and 0.6 μW for the 2 μm case for this frequency range.

References

1. J. R. Krenn, A. Dereux, J. C. Weeber, E. Bourillot, Y. Lacroute, J. P. Goudonnet, G. Schider, W. Gotschy, A. Leitner, F. R. Aussenegg, and C. Girard, Phys. Rev. Lett. **82**, 2590 (1999).
2. L. Yin, V. K. Vlasko-Vlasov, J. Pearson, J. M. Hiller, J. Hua, U. Welp, D. E. Brown, and C. W. Kimball, Nano Lett. **5**, 1399 (2005).
3. S. I. Bozhevolnyi, V. S. Volkov, E. Devaux, and T. W. Ebbesen, Phys. Rev. Lett. **95**, 046802 (2005).
4. D. M. Koller, A. Hohenau, H. Ditlbacher, N. Galler, F. Reil, F. R. Aussenegg, A. Leitner, E. J. W. List, and J. R. Krenn, Nat. Photonics **2**, 684 (2008).
5. S. I. Bozhevolnyi, V. S. Volkov, E. Devaux, J.-Y. Laluet, and T. W. Ebbesen, Nature **440**, 508 (2006).
6. L. Tang, S. E. Kocabas, S. Latif, A. K. Okyay, D.-S. Ly-Gagnon, K. C. Saraswat, and D. A. B. Miller, Nat. Photonics **2**, 226 (2008).
7. E. Verhagen, A. Polman, and L. (K.) Kuipers, Opt. Express **16**, 45 (2008).
8. A. Otto, Z. Phys. **216**, 398 (1968).
9. R. H. Ritchie, E. T. Arakawa, J. J. Cowan, and R. N. Hamm, Phys. Rev. Lett. **21**, 1530 (1968).
10. K. Tanaka and M. Tanaka, Appl. Phys. Lett. **82**, 1158 (2003).
11. R. Zia, M. D. Selker, P. B. Catrysse, and M. L. Brongersma, J. Opt. Soc. Am. A **21**, 2442 (2004).
12. F. Kusunoki, T. Yotsuya, J. Takahara, and T. Kobayashi, Appl. Phys. Lett. **86**, 211101 (2005).
13. L. Liu, Z. Han, and S. He, Opt. Express **13**, 6645 (2005).
14. D. F. P. Pile, T. Ogawa, D. K. Gramotnev, Y. Matsuzaki, K. C. Vernon, K. Yamaguchi, T. Okamoto, M. Haraguchi, and M. Fukui, Appl. Phys. Lett. **87**, 261114 (2005).
15. J. A. Dionne, H. J. Lezec, and H. A. Atwater, Nano Lett. **6**, 1928 (2006).
16. L. Chen, J. Shakya, and M. Lipson, Opt. Lett. **31**, 2133 (2006).
17. R. Yang, M. A. Abushagur, and Z. Lu, Opt. Express **16**, 20142 (2008).
18. G. Veronis and S. Fan, Opt. Express **15**, 1211 (2007).
19. J. Tian, S. Yu, W. Yan, and M. Qiu, Appl. Phys. Lett. **95**, 013504 (2009).
20. V. R. Almeida, Q. Xu, C. A. Barrios, and M. Lipson, Opt. Lett. **29**, 1209 (2004).
21. N. N. Feng, R. Sun, L. C. Kimerling, and J. Michel, Opt. Lett. **32**, 1250 (2007).
22. Z. Wang, N. Zhu, Y. Tang, L. Wosinski, D. Dai, and S. He, Opt. Lett. **34**, 1498 (2009).
23. Z. Han and S. He, Opt. Commun. **278**, 199 (2007).
24. R. A. Wahsheh, Z. Lu, and M. A. G. Abushagur, Opt. Express **17**, 19033 (2009).
25. S. E. Kocabas, G. Veronis, D. A. B. Miller, and S. Fan, Phys. Rev. B **79**, 035120 (2009).
26. K. F. Macdonald, Z. L. Samson, M. I. Stockman, and N. I. Zheludev, Nat. Photonics **3**, 55 (2009).